CHAPTER: V

DEVELOPMENT AND CHARACTERIZATION OF BIODEGRADABLE POLYVINYL ALCOHOL/CARBOXYMETHYL CELLULOSE COMPOSITE FILMS

5.1 Introduction

Synthetic polymers, originating from petrochemicals, have been associated with numerous environmental problems throughout their production and disposal processes [1]. Packaging constitutes a substantial portion of the world's plastic waste, greenhouse gas emissions, and climate change [2]. This has led to a heightened focus on creating bio-based materials as an environmentally friendly alternative to traditional synthetic plastics [3,4]. In packaging, polymers with excellent barrier, mechanical, optical, antimicrobial, thermal, and biodegradable properties are necessary to enhance the shelf life of products [5]. Researchers are increasingly exploring natural polymers derived from sources such as mucilage, plant gums, and proteins as sustainable and biodegradable alternatives to synthetic materials [6,7]. Biodegradable polymers have a wide range of applications across various fields, including pharmaceuticals, medicine, agriculture, consumer electronics, and particularly in packaging [8,9]. It also serves as a carrier for additives like antimicrobial agents (e.g., zinc oxide, titanium oxide, etc) and antioxidants (e.g., anthocyanins, essential oils, etc), making it suitable for different types advanced packaging systems [10]. Several renewable biopolymer sources, like chitosan, starch, polylactides, agarose, cellulose-based polymers, etc have been used as host polymers in the production of different polymer electrolyte systems [11-13].

Among many biopolymers, carboxymethyl cellulose (CMC) is a prominent biopolymer, derived from natural cellulose through chemical modification. It is semi-crystalline in structure, water soluble, non-toxic nature, biodegradability, and has outstanding film-forming properties that makes it highly valuable [14]. However, as a standalone polymer, it does face certain drawbacks, including significant stiffness and elongation at break of less than 8% [15]. Thus, to overcome the limitation of a single polymer system, hybrid polymer electrolyte blends have been researched extensively for a wide range of applications. The incorporation of additives such as polymers and nanomaterials proved to be more efficient for enhancing properties compared to the development of entirely new polymers with desired characteristics [16]. For polymer blending, thermoplastics such as polyolefins, polystyrene, polyester, nylon, polycarbonates, PLA, PVA, etc, are mostly preferred because they can be molded into desired shapes [17,18]. PVA stands out as a fossil-based water-soluble polymer that undergoes biodegradation and possesses advantages such as being flexible, non-toxic, suitable for water-based processes, and biocompatible [19]. It is also generally recognized as safe (GRAS) by regulatory standards, and PVA has received approval from the Food and Drug Administration (FDA) for its use in packaging applications [20]. Despite this, PVA has some limitations, i.e., low tensile strength, water-soluble, and minimum barrier properties [21]. To overcome the limitations of single polymer system, blending of polymers has proven to be a successful method for modifying the properties of polymeric materials in a constructive manner.

Thus, the primary objective of this research is to develop hybrid PVA/CMC polymeric film and to investigate the effect of different concentration of CMC biopolymer on film's physicochemical, mechanical, barrier, thermal, and antimicrobial properties. Additionally, soil degradation assessments are conducted to evaluate the degradation rate of the hybrid films. Furthermore, the findings have been validated with previous studies to ensure a comprehensive understanding of the results.

5.2 Experimental procedure

5.2.1 Development of PVA and PVA/CMC films

The details of the materials and reagents used for the development of films has been stated detailed in Chapter 3, under the materials and methodology section 3.1. Fabrication process was carried out using the solvent casting technique [22,23]. Initially, 3% (w/v) of PVA (3g) was dissolved in 100 ml distilled water at 90 °C and stirred for 3 hours at 600 rpm in a magnetic stirrer. A similar preparation was done for the development CMC of 0.5%-1.5% (w/v) solution. The polymer solutions were then mixed in 1:1 ratio, followed by addition of 1% (v/v) glycerol (1ml) and sonication for 15 minutes. A 2% (v/v) $CaCl_2$ (2ml) solution was then applied to the petri plates to facilitate the cross-linking of the mixed polymer solution. Subsequently, the solution was evenly spread across the petri dish and placed in a hot air oven maintained at 45 °C-50 °C for 36-40 hours. The films were then gently taken out and stored in a desiccator to protect them from moisture absorption. Figure 5.1 shows the schematic steps for the fabrication of polymeric films by solvent casting method. Figure 5.2. shows different compositions of PVA and PVA/CMC developed films.

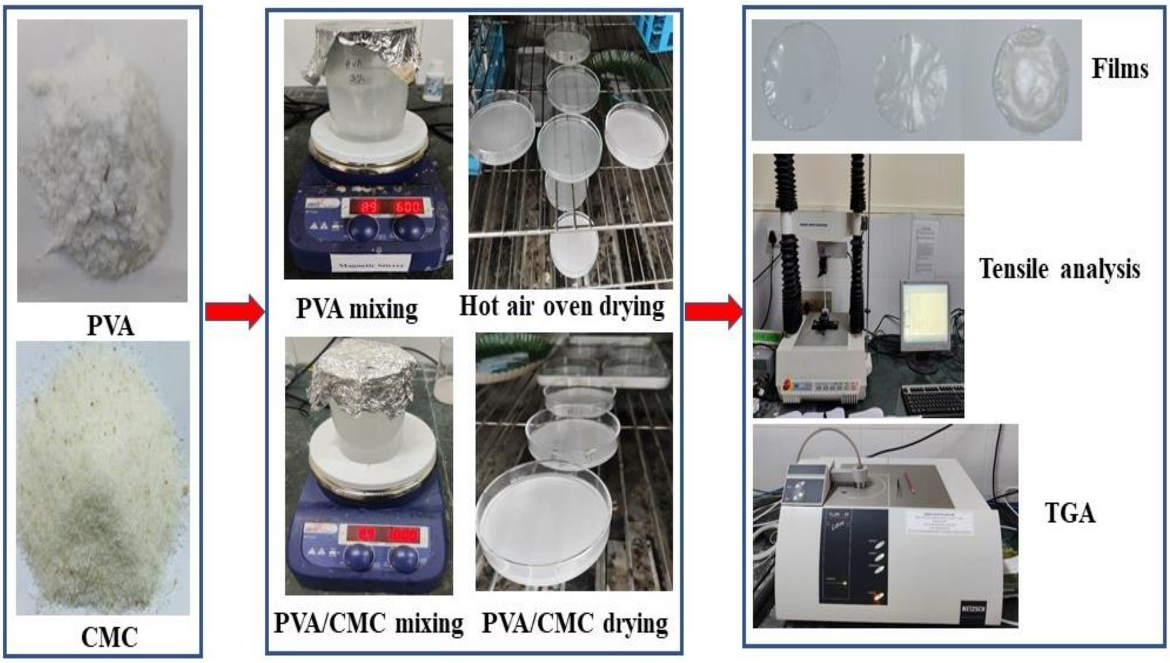

Figure 5.1. Schematic flowchart of diagram showing the fabrication of polymeric films

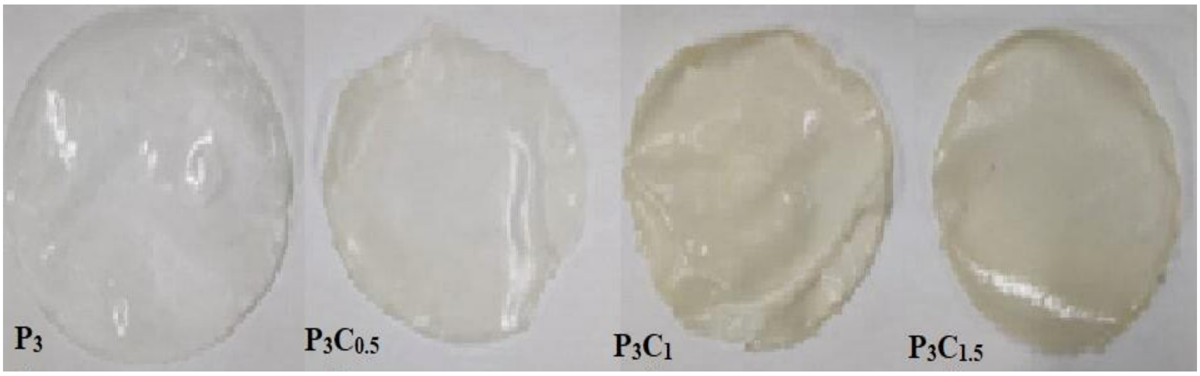

Figure 5.2 Developed films P_3: PVA; $P_3C_{0.5}$: PVA+0.5% CMC; P_3C_1: PVA+1% CMC, $P_3C_{1.5}$: PVA+1.5% CMC

5.3 Results and discussion

Physical, morphological, mechanical, light barrier, water vapor permeability, moisture retention capacity, thermal, anti-microbial and biodegradation properties of the films has been evaluated and discussed below.

5.3.1 Assessment of thickness, tensile properties, and SEM analysis

The thickness, tensile strength (TS), and elongation at break (EAB) of the films were evaluated and are shown in Table 5.1. A marginal change in the thickness was observed from P_3 to $P_3C_{1.5}$, approximately 0.79 mm to 0.84 mm. As shown in Table 5.1, the TS of the films ranged from 1.059 MPa to 1.401 MPa, while the %EAB varied between 325.54% and 374.87%. With the addition of CMC from 0.5 wt.%-1.5 wt.%, the TS decreased from 1.294 MPa to 1.059 MPa, while there was a notable increase in EAB from 275.86% to 374.87%. Film $P_3C_{1.5}$ showed the highest enhancement in EAB, approximately 15.15%, compared to P_3. The rise in tensile properties of PVA/CMC composite films is due to the formation of H-bond and increased cross-linked density into the polymer matrix system, promoting superior load transfer to the composite film. In line with existing literature, the %EAB of CMC-based film was found to be below 8% due to its stiff behaviour [15]. Thus, blending with PVA polymer confirmed an improvement in the EAB of a single polymer system. A comparable outcome was observed in PVA/CMC/ZnO membranes, where the TS and EAB were measured at 15.80 MPa and 179.0%, respectively [24].

Table 5.1 Physical and mechanical result of the films

Films	PVA wt.%	CMC wt.%	Film thickness (mm)	TS (MPa)	EAB (%)	WVP×10^{-5} (g/m.h. Pa)	% MRC
P_3	3	-	0.710± 0.005^a	1.401± 0.004^a	325.54± 3.92^a	8.06± 0.21^a	79.33± 0.05^a
$P_3C_{0.5}$	3	0.5	0.710± 0.003^b	1.294± 0.015^b	275.86± 3.87^b	4.94± 0.05^b	78.37± 0.09^b
P_3C_1	3	1	0.752± 0.006^c	1.137± 0.004^c	285.24± 8.03^c	6.18± 0.03^c	75.72± 0.26^c
$P_3C_{1.5}$	3	1.5	0.843± 0.004^d	1.059± 0.003^d	374.87± 1.78^d	7.36± 0.09^d	72.38± 0.66^d

Legend: The data is presented as Mean ± SD from three independent assays. The letters (a-d) in the respective columns indicate significant differences ($P \leq 0.05$).

Among the various CMC concentrations, $P_3C_{0.5}$ film containing 0.5 wt.% CMC exhibited the highest TS and enhanced WVP compared to the other hybrid films. These characteristics are essential for evaluating the film's mechanical strength and barrier performance. Consequently, SEM analysis was conducted on the $P_3C_{0.5}$ film to further investigate its morphological properties. The images of film $P_3C_{0.5}$ were captured before and after the tensile test, as depicted in Figure 5.3.

As seen in Figure 5.3 (a), minimum surface defects and continuous morphology was observed on the film’s surface. This correlates to the homogenized mixing of the polymer blends with strong H-bonds formation and increased crosslinking between PVA and CMC. Images also revealed a continuous microstructure of the film with less phase segregation, indicating the amorphous nature of the polymer blend. Figure 5.3 (b) shows the SEM image after the tensile test, in which development of furrows on the film’s surface is observed. The appearance of furrows in the longitudinal direction shows strong adherence to the polymer matrix and reflects the film's elongation in the tensile axis.

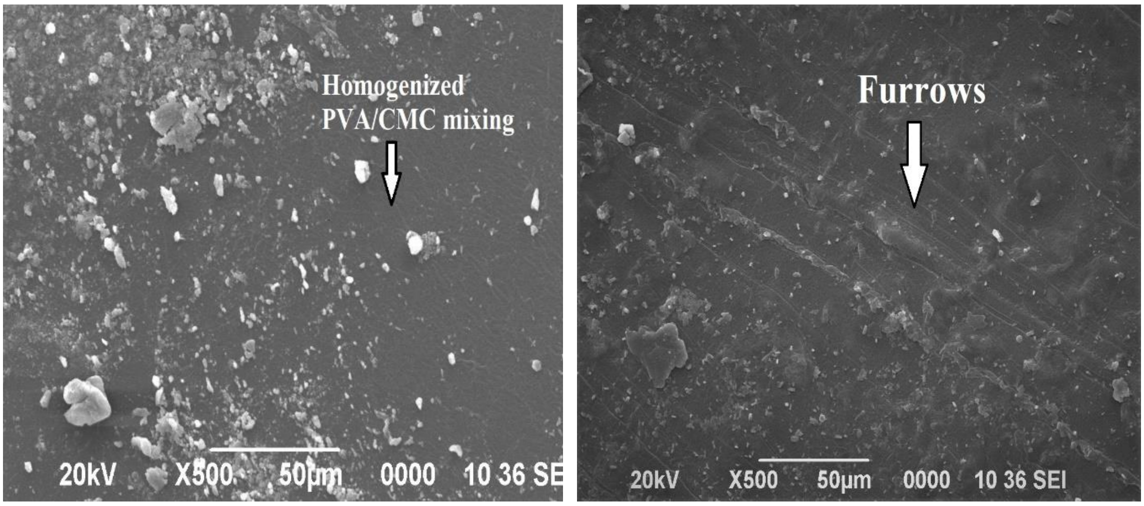

(a) Before tensile test (b) After tensile test

Figure 5.3 SEM micrographs of $P_3C_{0.5}$ film (a) before and (b) after tensile test

5.3.2 Water vapor permeability and moisture retention capacity

The water vapor permeability (WVP) and moisture retention capacity (MRC) are important properties of films used to manage moisture migration, ensuring the freshness and extending the shelf life of packaged food. According to Table 5.1, the WVP for P_3 film was measured approximately 8.06×10^{-5} g/m.h.Pa. In contrast, the hybrid PVA/CMC films exhibited a WVP ranging from 4.94×10^{-5} to 7.36×10^{-5} g/m.h.Pa. Notably, the lowest WVP was recorded for film $P_3C_{0.5}$ with 0.5 wt.% CMC concentration, which showed a reduction of 38.76% compared to the PVA film. The incorporation of CMC into the PVA matrix facilitates the formation of a hydrophilic network which traps the water molecules and reduce their mobility, further contributing to lower WVP [25]. The interaction between cellulose and PVA enhances the overall hydrophilicity of the film, which is essential for effective moisture control [21]. Moreover, crosslinking enhances the intermolecular interactions, such as H-bonding, between PVA and CMC chains, resulting in a more stable three-dimensional network compared to PVA film. The interaction decreases free space in the film, restricting water molecule diffusion [26]. Thus, blending of PVA with CMC showed improved barrier properties of the hybrid films, by forming a robust network that reduces WVP, promoting strong intermolecular interactions and crosslinking, thereby improving structural and barrier properties.

Table 5.2 Comparison table of previous literature with the present study

Polymer	Additives	WVP×10^{-5} (g/m.h.Pa)	TS (MPa)	%EAB	Reference
PHBV	CNC/GO	8.28	26	13	[27]
PVP-CS	GO	0.81	-	-	[28]
CMC	GnP	4.3	5.6	21	[29]
PVA	Au	-	1.45	34.79	[30]
SLPP	PVA/Starch	0.04	0.16	10.62	[23]
PVA	GO	6.76	1.51	268.64	[22]
PVA	CMC	4.94	1.29	275.86	Present study

MRC is determined by the loss of water vapor from the film. Table 5.1 displays the MRC of the films, ranging from 72.38% to 79.33%. It was observed that addition of CMC declines the MRC of the hybrid plastics. The hydrophilic characteristic of PVA and CMC results in the retention of water molecules within the matrix and facilitates the formation of H-bonds. This, in turn, diminishes the mobility of polymer chains and hinders the permeation of water molecules within the membrane. In accordance with prior research, the suggested MRC for food packaging films is between 78% and 95% [21,22]. This indicates that the MRC values observed in the developed films align with the recommended range for food packaging applications, showcasing its capability to retain moisture, and preventing moisture loss effectively.

A comparison study was made by referencing existing literature, and the findings were summarized in Table 5.2. It was found that the results of this study corresponded with those reported in previous research. Moreover, a significant enhancement in WVP values was noted when compared to findings from other studies.

5.3.3 Determination of thermal property

The thermal analysis of the films was assessed using TGA. The film's TGA and derivative thermogravimetric (DTG) curves are shown in Figure 5.4(a) and (b), respectively. These curves illustrate the % mass loss as well as the rate of mass loss over a range of temperatures. Figure 5.4(a) reveals three distinct stages of mass degradation for PVA and

PVA/CMC hybrid films. The initial stage mass loss occurring below 200 °C, involves moisture evaporation, while the second stage (250 °C-350 °C) corresponds to main chain degradation followed by polyene formation. The third stage, observed above 400 °C, involves the degradation of adjacent chains within the polymeric films [31]. For hybrid PVA/CMC films, the second step of mass decomposition resulted in the degradation of the carboxylate group, which is the characteristic structure of CMC. The final stage decomposition was attributed to the breakdown of remaining carbonaceous material and ash formation. As observed in the TGA graph, the thermograms of PVA/CMC exhibited lower weight loss compared to pure PVA. This difference arises from the pyrolysis process, during which the composite material undergoes thermal degradation, and releasing volatile products. However, due to the H-bond between PVA and CMC, more heat is needed to break this linkage, thus hindering the degradation process of volatile substances. Consequently, there is a reduced propagation of pyrolysis, resulting in an overall deceleration of the material's degradation.

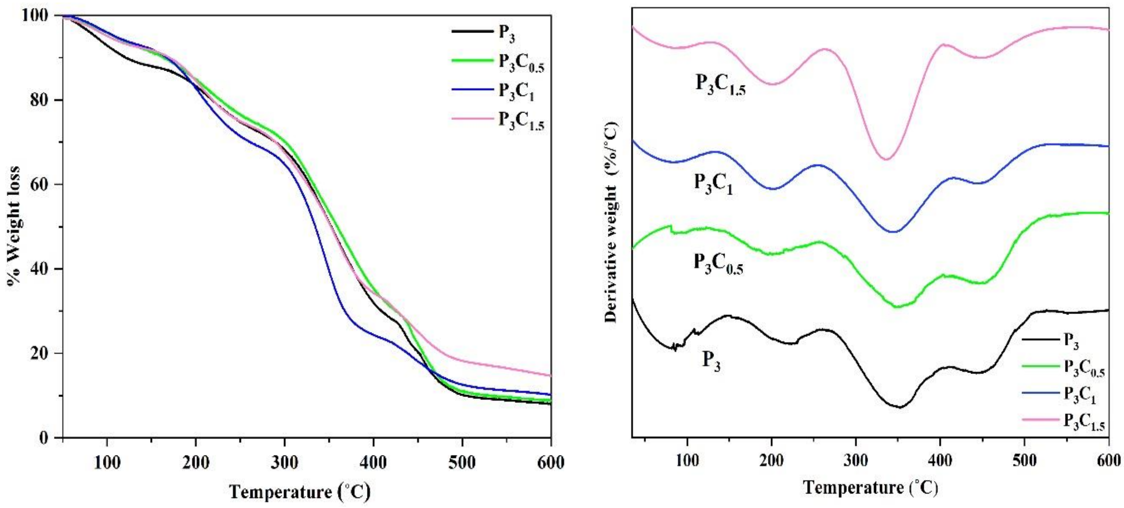

(a) TGA (b) DTG

Figure 5.4 (a)TGA and **(b)** DTG thermograph of developed films

The DTG curve, depicted in Figure 5.4(b), determines the rate of mass loss across a specified temperature. The polymer films exhibited primarily three stages of mass loss, where the initial decomposition step indicated a mass loss ranging from 5% to 15% for all the polymeric films. The second decomposition stage was characterized by a significant mass occurring at an onset temperature of 220 °C, accounting for approximately 55%-65%. During this stage, the rate of mass degradation for hybrid PVA/CMC films was 5%-8% lower as compared to the pure PVA film. At temperatures above 400 °C, the polymeric films experienced a significant mass loss of 25%-30%. Additionally, higher concentrations of CMC lead to the distortion of H-bonds at elevated temperatures. Distortion of H-bonds affects the properties of the polymer system, such as its thermal stability, mechanical strength, and water solubility. Therefore, it is important to consider the effect of CMC concentration while designing and processing hybrid films for specific applications that involve high-temperature conditions. The present result was thus validated with published literature i.e. PVA/CMC/CuO films, where the second and final decomposition was observed at onset temperature between 200 °C-400 °C and above 400 °C [21].

5.3.4 Determination of film's color, absorbance, and opacity

One of the most influential aspects of packaging design and customer satisfaction is the color of the film [23]. Table 5.3 represents the color parameters of the developed films.

Table 5.3 Film's color and opacity value

Films	**Color**			**Opacity**
	L^*	**a^***	**b^***	
P_3	88.38 ± 0.23^a	-0.493 ± 0.025^a	2.042 ± 0.030^a	0.301 ± 0.006^a
$P_3C_{0.5}$	83.29 ± 0.63^b	-0.160 ± 0.023^b	2.565 ± 0.050^b	0.956 ± 0.046^b
P_3C_1	80.60 ± 0.44^c	-0.151 ± 0.045^c	3.081 ± 0.131^c	1.146 ± 0.024^c
$P_3C_{1.5}$	77.26 ± 0.20^d	-0.127 ± 0.012^d	3.946 ± 0.006^d	1.413 ± 0.020^c

It is evident that the addition of CMC resulted in a significant variation ($P \leq 0.05$) in the color. The recorded values for L*, a*, and b* falls within the ranges of 77.26 to 88.38, -0.12 to -0.49, and 2.04 to 3.94, respectively. It was seen from Table 5.3 that P_3 exhibits the lightest tint among the films. However, with an increase in the concentration of CMC from 0.5 wt.% to 1.5 wt.%, there was a noticeable reduction in the lightness of the film. Consequently, film $P_3C_{1.5}$ recorded the lowest L* value in comparison to film P_3. The a* parameter of films ranging from P_3 to $P_3C_{1.5}$ displayed negative values, indicating a slight greenish tint. The b* values, progressing from film P_3 to $P_3C_{1.5}$, were recorded on the positive side and increased with the addition of CMC. The rise in the b* value signified an increase in yellowish tint, with film $P_3C_{1.5}$ exhibiting the highest b*. Thus, based on the experimental data, it can be affirmed that the addition of CMC polymer significantly altered the color of the films.

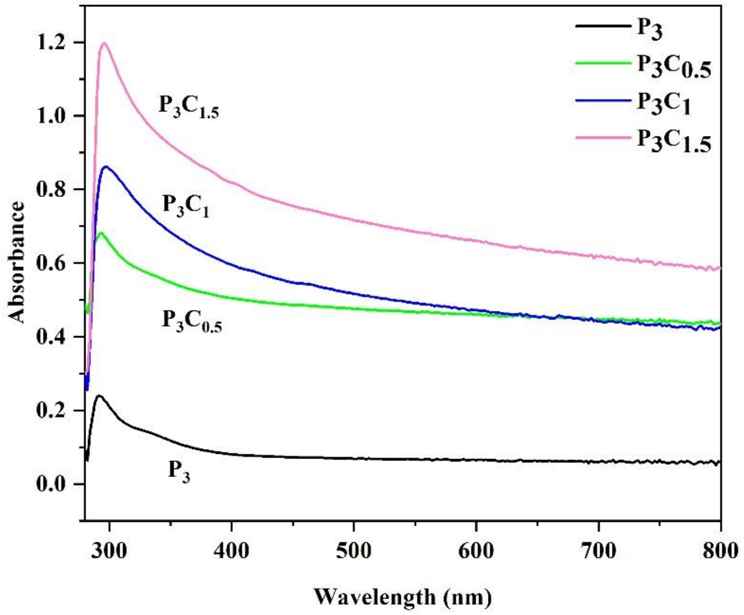

Figure 5.5 UV-Vis light absorbance of the films

Another essential property of film's design is the ability to block UV-Vis light. Figure 5.5 illustrates the absorption characteristics of the films across UV-Vis wavelengths. The absorption spectra display significant absorption of light in the UV range, around 300 nm, which are attributed to transitions in C=O bonds. Among the developed films, P_3 exhibit the least light absorbance, whereas it was increased from $P_3C_{0.5}$ to $P_3C_{1.5}$. Subsequently, the opacity of the films was evaluated and presented in Table 5.3. The opacity values ranged from 0.30 to 1.41 au ($P \leq 0.05$) for films P_3 to $P_3C_{1.5}$. A significant increment in opacity upto 218.83% and 371.86% was observed for film $P_3C_{0.5}$ to $P_3C_{1.5}$with respect to neat P_3. The addition of CMC resulted in an enhancement in the opacity of the hybrid films, reducing the passage of light through them. This highlights that hybrid PVA/CMC films have favourable absorption properties compared to PVA film, addressing the limitations of single-polymer film light barrier properties. Comparable results were noted for PVA/GO nanocomposite films, with opacity values ranging from 0.30 to 3.21, thereby supporting the findings of the present study [32].

5.3.5 FTIR

FTIR analysis was conducted to identify the structural features and ascertain the presence of important chemical groups along with their bonding within a polymer matrix. The FTIR spectra in Figure 5.6 showed six characteristic peaks between 1000 cm^{-1} to 4000 cm^{-1}. Sample P_3 displayed a significant absorption at 3431 cm^{-1}, which was associated with symmetric stretching and vibration of -OH groups [21]. Additionally, distinct absorbance peaks at 1033 cm^{-1}, 1382 cm^{-1}, 1466 cm^{-1}, 1645 cm^{-1}, 2927 were linked to C-O stretching, C-H vibration, CH_2 bending, H-O-H deformation, and -CH_2 stretching, respectively [33]. The absorbance between 1033 cm^{-1} to 1466 cm^{-1} indicates the presence of hydrocarbon (alkane) in PVA [34]. This revealed the important characteristics of PVA which was due to the vibration of carbon skeleton particularly related to C–H bending and C–O stretching [32]. These vibrational modes are essential for understanding the structural properties and interactions of PVA films, particularly their mechanical and thermal properties [35].

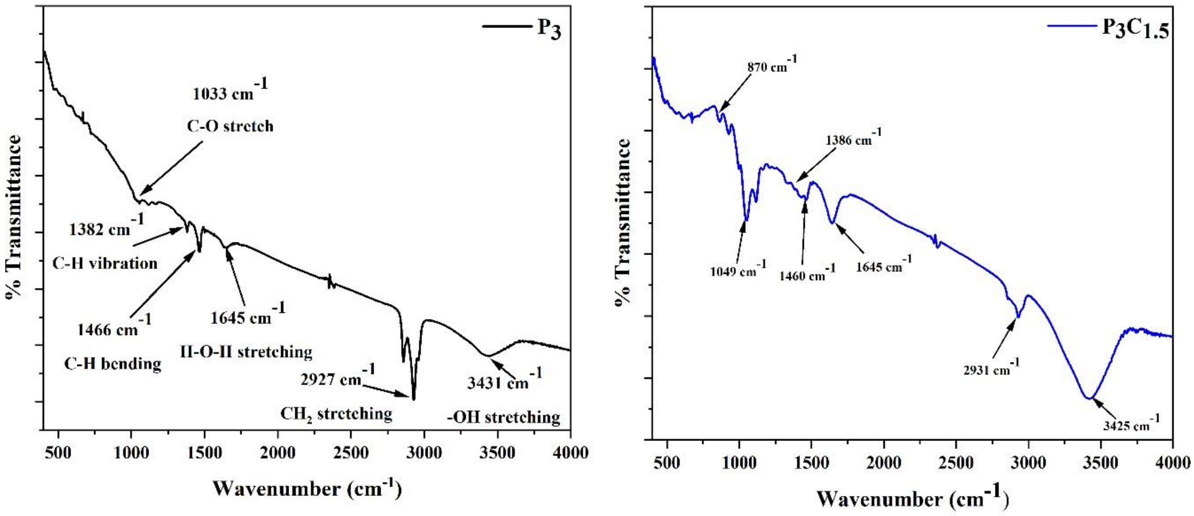

Figure 5.6 FTIR spectra of film (a) P_3 and (b) $P_3C_{1.5}$

Figure 5.6(b) demonstrates that addition of CMC to PVA modifies the absorption peaks, especially at 3425 cm^{-1}, which is linked to the stretching and vibrations of the -OH groups [36]. The absorbance peak at 1460 cm^{-1}, 1645 cm^{-1}, and 3425 cm^{-1} identified the existence of methyl, carboxyl, and hydroxyl functional groups, respectively [37]. The development of a new peak at 870 cm^{-1} is due to the vibration and stretching of C-C bonds. At 1033 cm^{-1} wavelength, C-O stretching was observed in film P_3, however for hybrid film $P_3C_{1.5}$, the absorption characteristic peak shifted to a higher wavelength to 1049 cm^{-1}. This indicates effective intermolecular interactions between PVA and CMC, where the semi-crystalline structure of PVA creates domains influenced by various processing parameters, including crosslinking. Crosslinking improves the physical and chemical properties of polymers by establishing covalent bonds between the polymer chains. The interaction between PVA and CMC is also evident in a slight shift of the -OH absorption band, indicating intramolecular forces between carboxylate and hydroxyl groups [21]. The shift validates the development of H-bonds with the -OH group, leading to narrowing and shifting of the band towards the lower wavenumber, from 3431 cm^{-1} to 3425 cm^{-1}. This demonstrates that the incorporation of CMC into the PVA polymer system results in strong interactions with PVA, thereby improving the amorphous nature and thermal resilience of the hybrid films.

5.3.6 Antimicrobial analysis

The assessment of the antibacterial activity of the films against *S. aureus* (gram-positive) and *E. coli* (gram-negative) bacteria was conducted by measuring the diameter of the inhibition zone. The antibacterial activity, determined through the disk diffusion method, is depicted in Figure 5.7 (a) and (b). It was noted that the developed film did not exhibit antibacterial properties, as evidenced by the absence of inhibition zones against both bacteria. The lack of inhibition zone indicates that the films do not have enough antibacterial activity to prevent the growth of the mentioned bacterial strains. The results suggest further modification or different formulations would be required to attain effective antibacterial activity in PVA/CMC films. Similar result was observed for antibacterial activity, with both PVA and PVA/CMC films showing no inhibition against *E. coli* and *Candida albicans* [21]. Incorporating GO nanofiller demonstrated effective antibacterial activity against *S. aureus* (gram-positive) bacteria, offering valuable insights into the potential use of nanomaterial in medical and packaging applications [22].

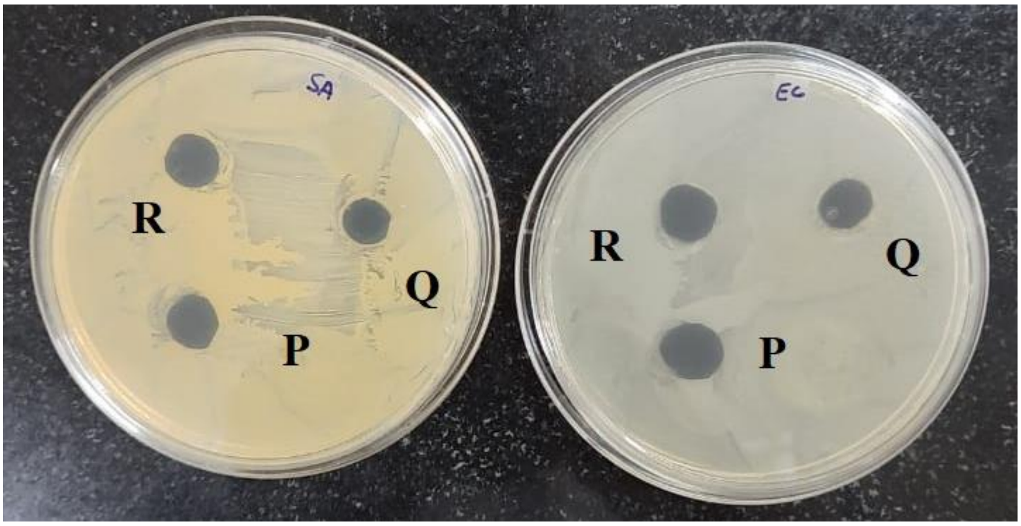

(a) *S. aureus* (b) *E. coli*

Figure 5.7 Antimicrobial activity by disk diffusion method (a) *S. aureus* (b) *E. coli*

5.3.7. Soil and microbial degradation

The results of biodegradability evaluation and the procedures conducted for soil burial analysis are depicted in Figures 5.8 and 5.9. Specifically, on the 10th day following the burial, PVA film demonstrated an approximate reduction in weight up to 8.42%. In comparison, the degradation of PVA/CMC-based films ranged between 10.54% to 11.76%.

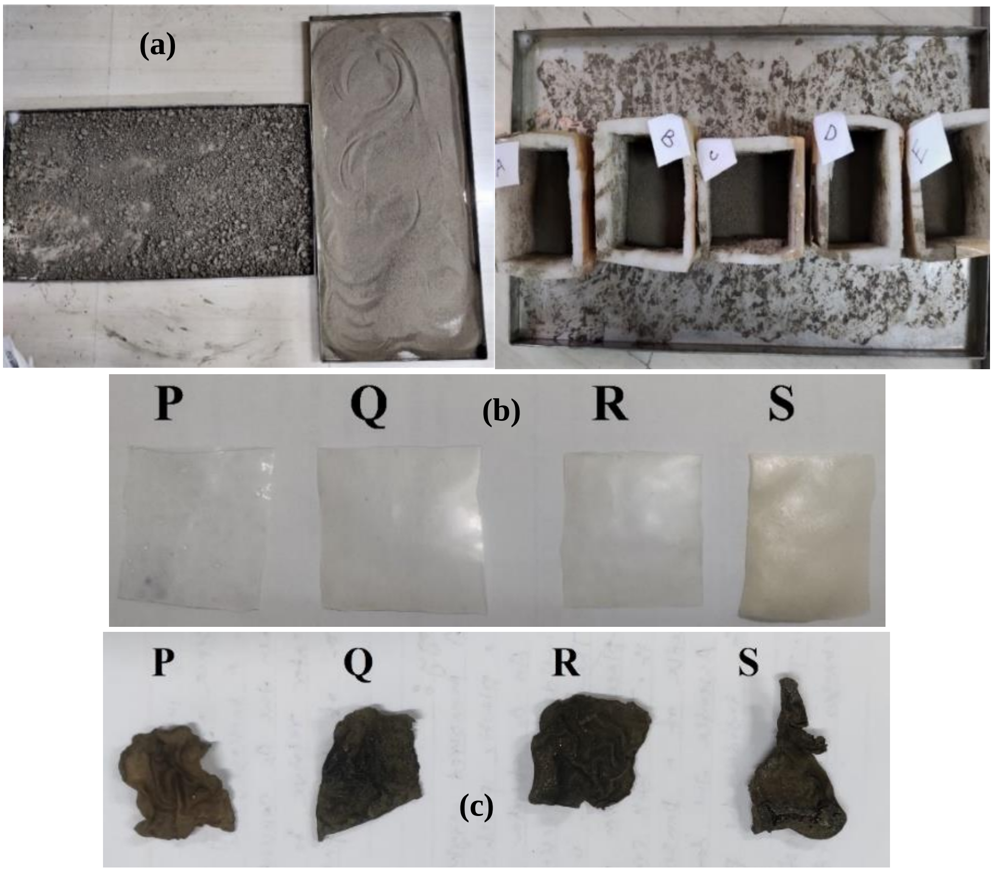

Figure 5.8 Soil burial analysis (a) soil preparation (b) films (3×3 cm) (c) 30th day films degradation result.

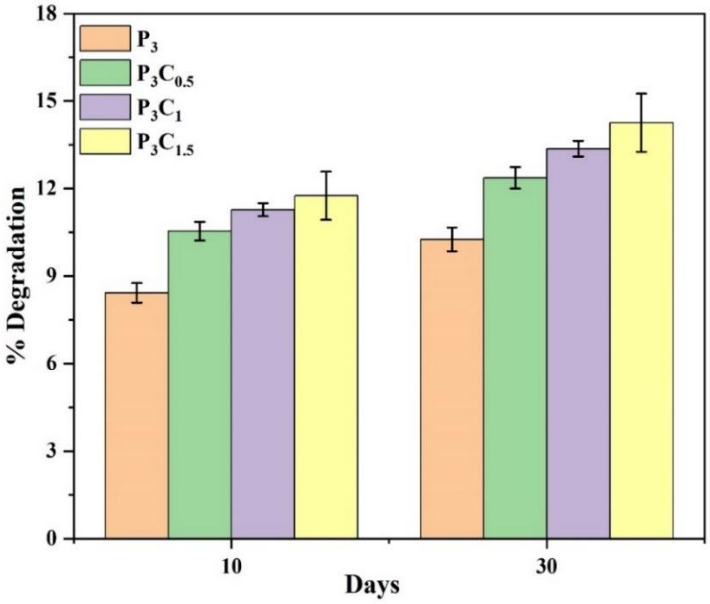

Figure 5.9 Soil burial degradation rate of films

By the 30th day, the weight reduction reached around 10.25% for PVA and 12.37% to 14.26% for PVA/CMC films. This shows an approximate increase in degradation rate up to 40% for the hybrid film. The test results demonstrate a direct correlation between burial time and the bioplastic degradation, with a proportional increase in biodegradation. Moreover, addition of CMC significantly accelerates the degradation with respect to PVA film. In the soil burial analysis, two-step degradation process is commonly observed. The initial step involves the adsorption of water molecules by the surface of the film, which leads to an increased swelling rate of the film. This, in turn, creates a favourable environment for microorganisms to proliferate on the film. The second phase comprises enzymatic breakdown, where bacteria cause damage to the polymeric network of the film, initiating the microbial degradation process [38].

Microorganisms play a key role in the breakdown of natural and synthetic and polymers [39]. However, understanding of the biodegradation of synthetic polymers is limited, likely due to their recent development and slower degradation rates in natural environments [40]. Polymers can serve as potential substrates for heterotrophic microorganisms such as bacteria and fungi. The biodegradability of polymers is influenced by factors such as crystallinity, molecular weight, and physical forms [41]. As the molecular weight of a polymer increases, its susceptibility to degradation by microorganisms decreases. High molecular weights often result in decreased solubility, making them less accessible for microbial attack. This is because bacteria typically require substrates to be assimilated through the cellular membrane before being further degraded by cellular enzymes. The most common microorganisms known to be able to break down PVA are aerobic bacteria, primarily those belonging to the genera *Alcaligenes*, *Bacillus*, and *Pseudomonas*. *Pseudomonas* species, in particular, were the initial bacteria discovered in soil samples with the ability to utilize PVA as their exclusive carbon source [42]. Thus, the microbial biodegradability test was carried out with modified ASTM G21-70, as depicted in Figure 5.10. For the present study, PVA, PVA/CMC0.5, PVA/GO, and synthetic plastic samples were taken into consideration. The experimental setup involved the utilization of bacterial strains, specifically *B. subtilis* and *P. putida*. At the commencement of the experiment on day 0, there was minimum microbial growth of *B. subtilis* and *P. putida* on both the bioplastic samples and agar media. However, by day 1, both bacterial strains-initiated growth by gradually covering the surface of the bioplastic material. Over the subsequent days, microbial proliferation continued, becoming increasingly evident by day 2. The agar media utilized in this experiment contained only minerals and did not include any supplementary carbon sources. As a result, the observed microbial growth attributes to the degradation of the bioplastic, in which microorganisms utilize them as a carbon source.

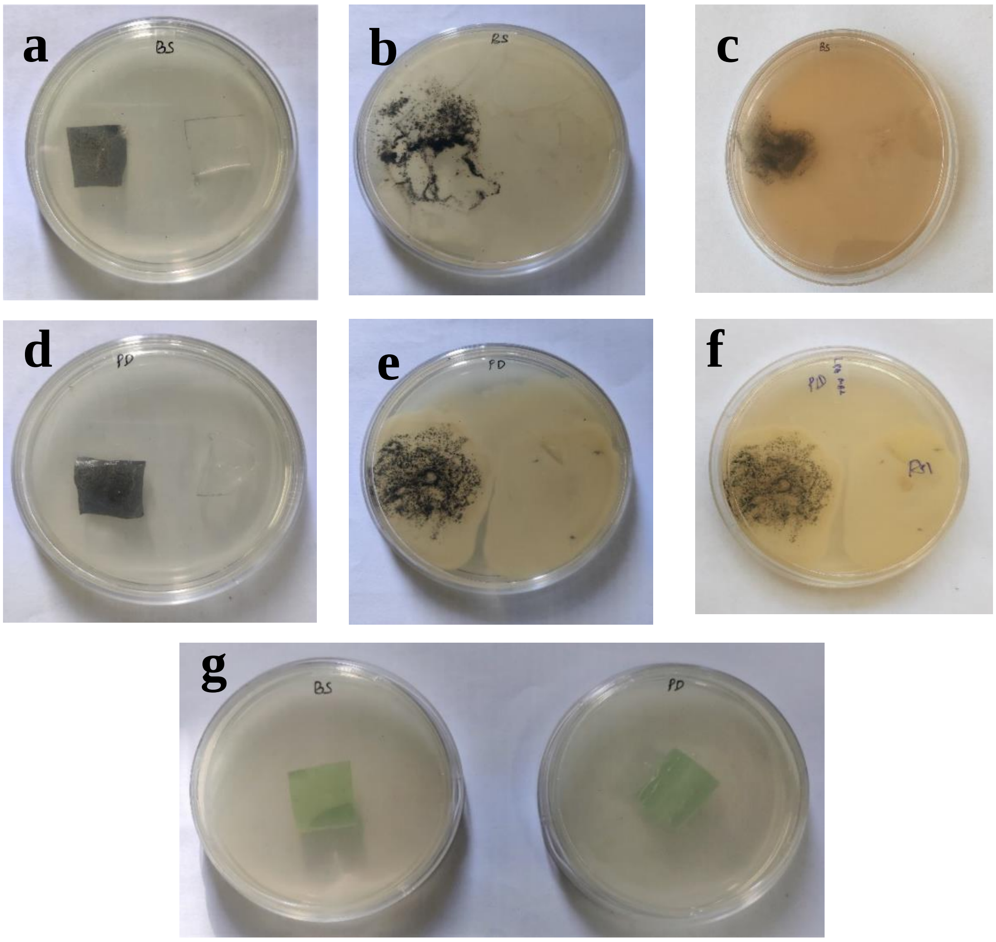

Figure 5.10 Biodegradation analysis against (a) *B. subtilis* day 0; (b and c) day 2, sample P_3 and $P_3Q_{0.5}$; (d) *P. putida* day 0; (e and f) day 2, sample P_3 and $P_3Q_{0.5}$; (g) negative control (synthetic plastic) day 2.

Throughout the degradation, microorganisms release exoenzymes that dismantle complex polymers, resulting in the production of shorter chains or smaller molecules such as oligomers, dimers, and monomers. These smaller molecules are sufficiently reduced in size to pass through the semi-permeable outer membranes of bacteria, where it can then be utilized as sources of carbon and energy. Several enzyme systems have been recognized for their role in facilitating the degradation of PVA. Within the enzyme systems, dehydrogenase or oxidase enzymes are responsible for initially breaking the primary carbon-carbon bonds within the polymer chain. Subsequently, hydrolase or aldolase enzymes follow this cleavage process. The types of microorganisms and the pathways they utilize for breaking down polymers are typically dictated by the prevailing environmental conditions. In oxygen-rich environments, aerobic microorganisms primarily drive the degradation of complex materials, ultimately resulting in microbial biomass, carbon dioxide, and water as the final by-products [43]. A comparative study was conducted on synthetic plastic as seen in Figure 5.10 (g), revealing no growth in the negative control. This observation suggested that synthetic plastic lacked nutritional value for bacterial growth, indicating its significant resistance to microorganisms. Similar observation of microbial degradation was seen for GO based PVA films [22]. Thus, from the present study it was concluded that the developed polymeric films undergo microbial degradation as compared to synthetic commercial plastic. These results emphasize the potential advantages of hybrid PVA/CMC bioplastics in comparison to single polymer systems. Thus, future research is likely to concentrate on integrating various nanoparticles or different fabrication process for its application in packaging and biomedical applications.

5.4 Conclusions

In the present study PVA based PVA/CMC hybrid polymeric films were developed by incorporating CMC at different concentrations (0.1%-1.5%). The effect of CMC on essential properties of the hybrid films such as physiochemical, mechanical, barrier, optical, thermal, morphological, antimicrobial, and biodegradation properties was observed. Some important findings from the present research work are as follows:

- Among the various formulations, the $P_3C_{0.5}$ film, which contains 0.5% CMC, demonstrated the highest TS and improved flexibility compared to other hybrid films.
- The addition of CMC led to improvements in WVP and MRC, with a notable 38.73% enhancement in WVP and an MRC of 78.37% at the 0.5% CMC concentration compared to pure PVA films.
- The hybrid films also exhibit enhanced light absorbance at UV wavelength with opacity ranging from 0.30 to 1.41.
- TGA analysis indicated that the decomposition temperature of PVA/CMC hybrid films was significantly higher than that of pure PVA films, resulting in reduced mass loss at elevated temperatures. The improvement suggests that CMC integration enhances the thermal stability of the films, making them more suitable for high-temperature applications.

- Additionally, FTIR analysis revealed that CMC incorporation leads to the formation of strong hydrogen bonds within the polymer blend, which positively influences the intermolecular forces in the cellulose matrix.
- The developed films did not exhibit antibacterial activity against *S. aureus* and *E. coli*, but demonstrated efficient microbial degradation when subjected to *B. subtilis* and *P. putida* bacteria.
- Moreover, incorporation of CMC accelerated the soil biodegradation rate of PVA films by approximately 40% over 30 days. These results demonstrate the potential of PVA/CMC hybrid films as sustainable packaging materials, combining durability, functionality, and environmental advantages. Future studies could focus on enhancing their antibacterial properties and refining formulations for targeted applications.

Bibliography

1. Kanatt, S. R. Active/smart carboxymethyl cellulose-polyvinyl alcohol composite films containing rose petal extract for fish packaging. *International Journal of Food Science and Technology*, 56(11): 5753–5761, 2021.

2. Kapila, K. and Kirtania, S. Development and characterization of biodegradable polyvinyl alcohol/carboxymethyl cellulose composite films. *Journal of Food Measurement and Characterization*, 19:2425–2437, 2025.

3. Suganthi, S., Vignesh, S., Sundar, J. K., and Raj, V. Fabrication of PVA polymer films with improved antibacterial activity by fine-tuning via organic acids for food packaging applications. *Applied Water Science*, 10(4):1–11, 2020.

4. Aznar, M., Ubeda, S., Dreolin, N., and Nerin, C. Determination of non-volatile components of a biodegradable food packaging material based on polyester and polylactic acid (PLA) and its migration to food simulants. *Journal of Chromatography A*, 1583:1–8, 2019.

5. Ahmed, I., Lin, H., Zou, L., Brody, A. L., Li, Z., Qazi, I. M., Pavase, T. R., and Lv, L. A comprehensive review on the application of active packaging technologies to muscle foods. *Food Control*, 82:163–178, 2017.

6. Kapila, K., Samanta, S., and Kirtania, S. Fabrication and characterization of ramie fiber based hybrid composites. In Pandey, K., Misra, R., Patowari, P., and Dixit, U., editors,

Recent Advances in Mechanical Engineering, pages 839-848. Springer-Singapore, 2021.

7. Marimuthu, S., Saikumar, A., and Badwaik, L. S. Development and characterization of biodegradable foam plates from corn starch and banana bunch stalks coated with beeswax. *Biomass Conversion and Biorefinery*, 15:7763-7777, 2025.

8. Dadkhah, H., Pirsa, S., Javadi, A., and Mohtarami, F. Biodegradable film based on sodium alginate/flax seed mucilage modified with norbixin and WO_3 nanoparticles: investigation of physicochemical properties and release of active substances. *Biomass Conversion and Biorefinery*, 14(15):17663–17675, 2024.

9. Shabkhiz, M. A., Pirouzifard, M. K., Pirsa, S., and Mahdavinia, G. R. Alginate hydrogel beads containing thymus daenensis essential oils/glycyrrhizic acid loaded in β-cyclodextrin. Investigation of structural, antioxidant/antimicrobial properties and release assessment. *Journal of Molecular Liquids*, 344:117738, 2021.

10. Pirsa, S., Mahmudi, M., and Ehsani, A. Biodegradable film based on cress seed mucilage, modified with lutein, maltodextrin and alumina nanoparticles: Physicochemical properties and lutein-controlled release. *International Journal of Biological Macromolecules*, 224:1588–1599, 2023.

11. Pirsa, S. and Mohammadi, B. Conducting/biodegradable chitosan-polyaniline film; Antioxidant, color, solubility and water vapor permeability properties. *Main Group Chemistry*, 20(2):133–147, 2021.

12. Nasiri, S. L., Azizi, M. H., Movahedi, F., Rahimifard, N., and Tavakolipour, H. Potential perspectives of CMC-PET/ZnO bilayer nanocomposite films for food packaging applications: physical, mechanical and antimicrobial properties. *Journal of Food Measurement and Characterization*, 15(4):3731–3740, 2021.

13. Junaid, P. M., Saikumar, A., Nazim, M. S., Zaidi, S., Badwaik, L. S., and Ahmad, F. Film-based packaging for food safety and preservation: issues and perspectives. In Ahmad, F., Mohammad, Z.H., Ibrahim, S.A., Zaidi, S., editors, *Microbial Biotechnology in the Food Industry*, pages 429-446, Springer, Cham, 2024.

14. Hashmi, M., Ullah, S., Ullah, A., Saito, Y., Haider, M. K., Bie, X., Wada, K., and Kim, I. S. Carboxymethyl cellulose (CMC) based electrospun composite nanofiber mats for food packaging. *Polymers,* 13(2):302, 2021.

15. Nasibi, S., Khoramabadi, H. N., Arefian, M., Hojjati, M., Tajzad, I., Mokhtarzade, A., Mazhar, M., and Jamavari, A. A review of polyvinyl alcohol / carboxymethyl cellulose (PVA/CMC) composites for various applications.*Journal of Composites and Compounds,* 2(3):69–76, 2020.

16. Yorghanlu, R. A., Hemmati, H., Pirsa, S., and Makhani, A. Production of biodegradable sodium caseinate film containing titanium oxide nanoparticles and grape seed essence and investigation of physicochemical properties. *Polymer Bulletin*, 79(10):8217–8240, 2022.

17. Abdolsattari, P., Bari, M. R., and Pirsa, S. Smart film based on polylactic acid, modified with polyaniline/ZnO/CuO: Investigation of physicochemical properties and its use of intelligent packaging of orange juice. *Food and Bioprocess Technology*, 15(12):2803–2825, 2022.

18. Abdullah, Z. W., Dong, Y., Davies, I. J., and Barbhuiya, S. PVA, PVA blends, and their nanocomposites for biodegradable packaging application. *Polymer-Plastics Technology and Engineering*, 56(12):1307–1344, 2017.

19. Marusincova, H., Husarova, L., Ruzicka, J., Ingr, M., Navratil, V., Bunkova, L., and Koutny, M. Polyvinyl alcohol biodegradation under denitrifying conditions. *International Biodeterioration & Biodegradation*, 84:21–28, 2013.

20. Youssef, H. F., El-Naggar, M. E., Fouda, F. K., and Youssef, A. M. Antimicrobial packaging film based on biodegradable CMC/PVA-zeolite doped with noble metal cations. *Food Packaging and Shelf Life*, 22:100378, 2019.

21. Amaregouda, Y., Kamanna, K., and Gasti, T. Biodegradable polyvinyl alcohol/carboxymethyl cellulose composite incorporated with l-alanine functionalized MgO nanoplates: Physico-chemical and food packaging features. *Journal of Inorganic and Organometallic Polymers and Materials*, 32(6):2040–2055, 2022.

22. Kapila, K., Kirtania, S., Devi, L. M., Saikumar, A., Badwaik, L. S., and Rather, M. A. Potential perspectives on the use of poly (vinyl alcohol)/graphene oxide nanocomposite films and its characterization. *Journal of Food Measurement and Characterization*, 18(2):1012–1025, 2024.

23. Singha, P., Rani, R., and Badwaik, L. S. Sweet lime peel-, polyvinyl alcohol- and starch-based biodegradable film: preparation and characterization. *Polymer Bulletin*, 80(1):589–605, 2023.

24. Helmiyati, H., Hidayat, Z. S. Z., Sitanggang, I. F. R., and Liftyawati, D. Antimicrobial packaging of ZnO–Nps infused into CMC–PVA nanocomposite films effectively enhances the physicochemical properties. *Polymer Testing*, 104:107412, 2021.

25. Hu, D., Qiang, T., and Wang, L. Quaternized chitosan/polyvinyl alcohol/sodium carboxymethyl cellulose blend film for potential wound dressing application. *Wound Medicine*, 16:15–21, 2017.

26. Ghanbarzadeh, B., Almasi, H., and Entezami, A. A. Improving the barrier and mechanical properties of corn starch-based edible films: Effect of citric acid andcarboxymethyl cellulose. *Industrial Crops and Products*, 33(1):229–235, 2011.

27. Li, F., Yu, H. Y., Wang, Y. Y., Zhou, Y., Zhang, H., Yao, J. M., Abdalkarim, S. Y. H., and Tam, K. C. Natural biodegradable poly (3-hydroxybutyrate- co-3-hydroxyvalerate) nanocomposites with multifunctional cellulose nanocrystals/graphene oxide hybrids for high-performance food packaging. *Journal of Agricultural and Food Chemistry*, 67(39):10954–10967, 2019.

28. Mahmoudi, N., Ostadhossein, F., and Simchi, A. Physicochemical and antibacterial properties of chitosan-polyvinylpyrrolidone films containing self-organized graphene oxide nanolayers. *Journal of Applied Polymer Science*, 133(11), 43194, 2016.

29. Ebrahimzadeh, S., Ghanbarzadeh, B., and Hamishehkar, H. Physical properties of carboxymethyl cellulose based nano-biocomposites with Graphene nano-platelets. *International Journal of Biological Macromolecules*, 84:16–23, 2016.

30. Chowdhury, S., Teoh, Y. L., Ong, K. M., Rafflisman Zaidi, N. S., and Mah, S. K. Poly(vinyl) alcohol crosslinked composite packaging film containing gold nanoparticles on shelf life extension of banana. *Food Packaging and Shelf Life*, 24:100463, 2020.

31. Abu Hurayra–Lizu, K. M., Bari, M. W., Gulshan, F., and Islam, M. R. GO based PVA nanocomposites: tailoring of optical and structural properties of PVA with low percentage of GO nanofillers. *Heliyon*, 7(5):e06983, 2021.

32. Kharazmi, A., Faraji, N., Hussin, R. M., Saion, E., Yunus, W. M. M., and Behzad, K. Structural, optical, opto-thermal and thermal properties of ZnS–PVA nanofluids synthesized through a radiolytic approach. *Beilstein Journal of Nanotechnology*, 6:529–536, 2015.

33. Qua, E. H., Hornsby, P. R., Sharma, H. S. S., Lyons, G., and Mccall, R. D. Preparation and characterization of poly (vinyl alcohol) nanocomposites made from cellulose nanofibers. *Journal of Applied Polymer Science*, 113(4):2238–2247, 2009.

34. Elgharbawy, A. S., El Demerdash, A. G. M., Sadik, W. A., Kasaby, M. A., Lotfy, A. H., and Osman, A. I. Enhancing the biodegradability, water solubility, and thermal properties of polyvinyl alcohol through natural polymer blending: An approach toward sustainable polymer applications. *Polymers*, 16(15):2141, 2024.

35. Riaz, U., and Ashraf, S. M. Characterization of polymer blends with FTIR spectroscopy. In Thomas, S., Grohens, Y., and Jyotishkumar, P., editors, *Characterization of Polymer Blends: Miscibility, Morphology, and Interfaces*, pages 625-678, Wiley-VCH

Verlag GmbH & Co. KGaA, 2015.

36. Abead, S. H., Hadi Al-Kadhemy, M. F., and Abbas, K. N. Study physical characteristics of Polyvinyl Alcohol/Carboxymethyl cellulose blend films. *Kuwait Journal of Science*, 50(3B):1–14, 2023.

37. Arshad, M., Neelam, A., Haleem, N., Jamal, Y., Hina, K., Bilal, M., Shah, S. H., Hussain, I., and Zhang, Y. Synthesis and characterization of CMC/PVA/PVP composite microfiltration membrane. *Desalination and Water Treatment*, 203:70–79, 2020.

38. Roohi, Bano, K., Kuddus, M., Zaheer, M. R., Zia, Q., Khan, M. F., Ashraf, G. Md., Gupta, A., and Aliev, G. Microbial enzymatic degradation of biodegradable plastics. *Current Pharmaceutical Biotechnology*, 18(5): 429–440, 2017.

39. Gu, J. D. Biodegradability of plastics: the issues, recent advances, and future perspectives. *Environmental Science and Pollution Research*, 28(2):1278–1282, 2021.

40. Gu, J. D. On environmental biotechnology of bioremediation. *Applied Environmental Biotechnology*, 5(2): 28–33, 2021.

41. Gao, L. and Gu, J. D. A new unified conceptual framework involving maintenance energy, metabolism and toxicity for research on degradation of organic pollutants. *International Biodeterioration & Biodegradation*, 162:105253, 2021.

42. Chiellini, E., Corti, A., D’Antone, S., and Solaro, R. Biodegradation of poly (vinyl alcohol) based materials. *Progress in Polymer Science*, 28(6):963–1014, 2003.

43. Gu, J. D., Ford, T., Mitton, B., and Mitchell, R. Research on biodeteriotration of plastics. *International Biodeterioration & Biodegradation*, 186:105699, 2024.